International Journal of Advanced Research and Review

www.ijarr.in

URANIUM IONS REMOVAL FROM AQUEOUS MEDIA USING GRAPHENE OXIDE DERIVED FROM BLACK CARBON

Khaled A. Abd El-Rahem[1], Mahmoud A. Taher[1], Mohamed F. Cheira[2]

[1]Chemistry Department, Faculty of Science, Al-Azhar University, Assiut 71524, Egypt.
[2]Nuclear Materials Authority, P.O. Box 530, Maadi, Cairo, Egypt
*** Corresponding Author:** mf.farid2008@yahoo.com

ABSTRACT

Graphene oxide (GO) was prepared from black carbon by the Hummers method. The prepared GO was characterized by Scanning electron microscopy (SEM), Energy dispersive spectroscopy (EDX), Brunner-Emmett-Teller (BET) surface area analyzer, and Fourier transform infrared spectroscopy (FTIR). Go was used for U(VI) adsorption of Uranium ions from the acid solution. The effects of environmental settings on U(VI) adsorption were studied, including pH, contact time, adsorbent dose, initial concentration of U (VI), and temperature. The experimental results showed that the best uptake of uranium ions on Go adsorbent is 68.0 mg/g at pH 4, and150 mg/L initial U(VI) concentration for 50 min contact time at room temperature. The kinetic data fitted well with the pseudo-second-order kinetic model. Langmuir's adsorption model described the adsorption isotherm while the adsorption process was non-spontaneous, randomness, and exothermic. Also, the graphene oxide adsorbent was truly regenerated by 0.8M H_2SO_4 and 1:50 S:L ratio for 60 min contact time. Seven cycles of adsorption-desorption experiments were conducted to study the practical applicability and recurrent use of graphene oxide as an adsorbent.

Keywords: Black Carbon, Graphene Oxide, Uptake, Uranium Adsorption, Acid Solution.

1. INTRODUCTION

Uranium ions may come into the environment via application, manufacture, and uranium mining, which lead to hazards to human health and the ecological environment due to radioactivity and chemical toxicity (Cheira et al., 2017; Chen and Wang, 2016). However, with the extensive utilization of nuclear energy and other applications, the uranium is highly liberated into the liquid solutions as hexavalent ions, which threaten environmental safeguard and ecological balance (Atia et al., 2018; Sakr et al., 2018). Consequently, the elimination and extraction of U(VI) from aqueous solutions are crucial to nuclear energy generation and environmental safeguard (Hu et al., 2017; Yao et al., 2018; Liu et al., 2018).

In the past few decades, various approaches were applied for removal and recovery of U(VI), including, ion exchange (Cheira et al., 2014a; Zidan et al., 2020; Cheira, 2015a; Gado et al., 2019; Atia et al., 2021), precipitation (Duff et al., 2002),solution extraction (Cheira, 2020a), membrane separation (Zhou et al., 2014), adsorption (Cheira, 2015b; Abdien et al., 2016a; Cheira, 2019; Cheira et al., 2020a; Jiao et al., 2017). Adsorption is typically used to eliminate radionuclides from aqueous sources due to its high performance, low cost, and abounding adsorbents. Different graphene-based adsorbents, including graphene, graphene oxide, and various solid adsorbed materials (Cheira et al., 2019a; Zong et al., 2013; Atia et al., 2021;

Hassanin et al., 2019), were extensively examined as inherent adsorbents due to their unique physicochemical properties, such as chemical strength, structural variability, and low density. Adsorption mechanisms are widely governed by the properties of adsorbents, the physicochemical characteristics of contaminants, and the setting of adsorbate quality requirements (Abdien et al., 2016b; Li et al., 2015; Cheira et al., 2020b).

Recently, graphene-related materials and graphene oxide were fabricated extensively and used in numerous applications (Sanchez et al., 2012). At present, most GO was made by the exfoliation and chemical oxidation of graphite using the Hummers method (Zaaba et al., 2017). Since numerous oxygen-containing functional groups (e.g., carboxyl, carbonyl groups, and hydroxyl and epoxy groups) existed in the graphitic backbone of GO (Kim et al., 2010), they might be described as a highly oxidized form of graphene. They were attractive candidates for adsorption applications and were well-suited to the adsorption of both inorganic, heavy metal (Dong et al., 2016; Li et al., 2012; Wang and Chen, 2015), and organic contaminants (Cheng et al., 2013; Liao et al., 2019) due to their high oxygen-containing surface functionalities, large surface areas, and relatively high hydrophilicity.

To determine the degree of removal of inorganic and organic contaminants by graphene- oxide, it is necessary to understand the interactions between graphene oxide and pollutants, such as π-π bonding, hydrogen bonding, hydrophobic interactions, and electrostatic interactions (Cheng et al., 2012; Chowdhury and Balasubramanian, 2014). The properties of the contaminants influenced the removal of pollutants from aqueous solution using graphene oxide (e.g., inorganic/heavy metal or organic, size/shape, functional group(s), hydrophobicity, and pKa), as well as the properties of the adsorbent itself (e.g., charge, shape, functional group(s), and hydrophobicity) and water quality (e.g., solute concentrations, background ions, natural organic matter (NOM), pH, and temperature) (Wang et al., 2013; Kim et al., 2018; Sayed et al., 2020).

The purpose of this work was to prepare graphene oxide from black carbon by the Hummers method. The prepared graphene oxide was applied to remove uranium ions from the sulfate solution. The different experimental parameters, such as solution pH, contact time, adsorbent dose, initial uranium ions concentration, and temperature, were estimated by batch technique.

2. MATERIALS AND METHODS

2.1 Characterization

Uranium ions were determined by double on a JANEWAY UV/Vis 6405 spectrophotometer at 655.0 nm using Arsenazo III that used as chromophore (Marczenko and Balcerzak, 2000). Furthermore, a scanning electron microscope equipped with energy dispersive spectroscopy (SEM-EDX) was used to describe the morphologies of the prepared graphene oxide before and after adsorption. It was obtained from Philips XL 30.The studied adsorbent is also characterized using Fourier transform infrared spectrophotometer (FTIR, Shimadzu I.R. Prestige–21) controlled by IR resolution Software. FTIR analysis was performed using a KBrbeam splitter with 4000~400 cm1 wave number with a 4 cm^{-1}resolution.

2.2 Chemicals and Reagents

All chemicals and reagents were of analytical grade and could be used without further purification. Uranyl acetate dihydrate ($UO_2(CH_3COO)_2.2H_2O$, 99%), H_3PO_4 (85%), Arsenazo III (99%),and $NaNO_3$ (99%) were acquired from Merch, Germany. Ferrous sulfate ($FeSO_4.7H_2O$), sodium hydroxide (NaOH), sulfuric acid (98%), and H_2O_2 (30%) were gained from Sigma

Aldrich. Methanol, ethyl acetate were purchased from Scharlau Chemie, Spain. The black carbon was obtained from Birla Carbon Egypt SAE, Egypt.

2.3 Synthesis of Graphene Oxide

The black carbon was used to obtain nano-graphene oxide by the Hummer method (Zaaba et al., 2017). Concisely, black carbon (15 g) and$NaNO_3$ (10 g) were put into a 2L flask. The acid mixture of 250 mL H_2SO_4 (98%) and 65 mL H_3PO_4 (85%) was added into a flask under agitation, and the mixtures were cooled to 0–4 °C in an ice water bath. After that, $KMnO_4$ (18 g) was regularly added above100 min with violent agitating and cooling to ensure the temperature of the mixtures below 15 °C for 30 - 120 min. The mixture was heated to 33 °C ± 2 °C in a water bath till become pasty brownish grey colored for 12 hours. Then 300 mL distilled water was slowly added, and the mixtures were agitated for 20 min with continuous stirring at below95 °C. Large quantities of water (900 mL) and 45 mL H_2O_2 (30%) were added into the above mixture for 30 hours, stirring to terminate the reaction that results in a bright yellow color of the mixture. Then, the mixture was washed with 40 mL HCl (15%) to remove the remaining metal ions and centrifuged and washed several times to remove the acid. After that, a 30 min centrifugation process at 3000 rpm was conducted to remove any aggregates. Filtrate under vacuum and wash with ionized H_2O several times, then leave it in the dry oven at 90 °C. Finally, the resultant product (GO) was dried in a vacuum oven near 50 °C for around 24 hours. The suggested preparation processes of GO were set in Figure 1.

Figure -1: The suggested physical and chemical processes for GO preparation.

32.4 Uranium Adsorption Studies

In the present work, uranium ions' adsorption from their solutions was applied using the batch method. To study U(VI) adsorption, a series of experiments were conducted to determine the optimum conditions of the relevant factors controlling the adsorption process, such as pH, contact time, adsorbent dose, initial uranium concentration, and temperature. All the experiments were performed in duplicate, and the mean value is used in all cases.

The sorption experiments were carried out by mixing 50 mL of different initial uranium concentrations with (10-100mg) adsorbent dose in 100 mL conical flasks at 200 rpm mechanical shaker and different contact time varying from 5 to 120 min at different temperatures. The pH was studied by ranging from 1 to 6, whereas the pH was adjusted using 1M NaOH or 1M H_2SO_4 solutions. After filtration, the amount of uranium ions uptake was calculated by the difference between the equilibrium concentration and the initial concentration. On the contrary, the corresponding experiments attained the adsorption kinetics, equilibrium isotherms, and thermodynamic parameters.

From each adsorption experiment, uranium ions were adsorbed on the prepared adsorbent, the sorption capacity q_e (mg/g) and distribution coefficient (K_d) were evaluated from the following equations:

$$q_e = (C_0 - C_e)\, x \frac{V}{m} \quad (1)$$

$$K_d = \left(\frac{C_0 - C_e}{C_e} \right) x \frac{v}{m} \quad (2)$$

Where C_o and C_e are the initial and equilibrium metal ions concentrations (mg/L), respectively, v is the volume of the solution (mL), and m is the dry adsorbent weight (g).

3. RESULTS AND DISCUSSION

3.1 Characteristics of Graphene Oxide

A scanning electron microscope (SEM) is the most reliable and convenient device for studying the physical structure of the solid adsorbent. The SEM was also appropriated to investigate the change of surface and physical formations of GO and U/GO.As exhibited in Figure 2a,b, the surface of GO has smoothly formed by several holes (Figure 2a). After the adsorption of U(VI) on GO, the SEM picture indicated that the pores were filled with U(VI), and also the surfaces were smooth and agglomerate with uranium ions (Figure 2b). The semi-quantitative analysis of GO, and U/GO, were given in EDX spectra (Figure 2c,d). From the results in Figure 2c, the nitrogen, carbon, and oxygen peaks were presented in the spectrum of GO, and no other peaks were detected. After uranium ions adsorption on the GO adsorbent, it was clearly observed in Figures 2dthat was distinct peaks of uranium ions on the spectrum. The uranium peaks were perceived and confirmed U(VI) adsorption on GO.

Fourier transform infrared (FTIR) spectroscopy is a required analysis method that identifies several unique functional groups standing at the surface of the studied adsorbent. At the interaction of infrared light with solid materials, the chemical bond will expand, contract or bend. As a result, each functional group tends to absorb infrared radiation with a specific wave

number range regardless of the molecules' support structure. The GO, and U/GO, in Figure 3a,b were characterized by FTIR spectroscopy. The prepared graphene oxide (GO) exhibited broad absorption band at 3425 cm^{-1} that matched to -OH group stretching vibration. The vibration peak at 1632 cm^{-1} demonstrated the aromatic C=C or -OH of adsorbed water on GO, but the peak at 1700 $cm^{-1}$was exhibited to the C=O stretching peak of –COOH groups (Cheira et al., 2019b). The peak at 1419 $cm^{-1}$was recognized as -OH of deformation peak. The relatively broad peak at 1180 cm^{-1} and 955 $cm^{-1}$was indicated C–O of the epoxy group, and the 1099 $cm^{-1}$is due to C–O of the carboxyl group. After U(VI) adsorption, the –OH, and C=O, stretching vibration bands for the studied adsorbent were reduced and shifted to red shift with 5-10 cm^{-1}, which might be owing to the pickup of U(VI) to the surface adsorbent as shown in the spectra of U/GO (Figures 3b). Moreover, the new peaks of (O=U=O) near the 974 and 894 cm^{-1}(Suet al., 2021) of GO. This means that the uranyl cations react with -OH and epoxy groups.

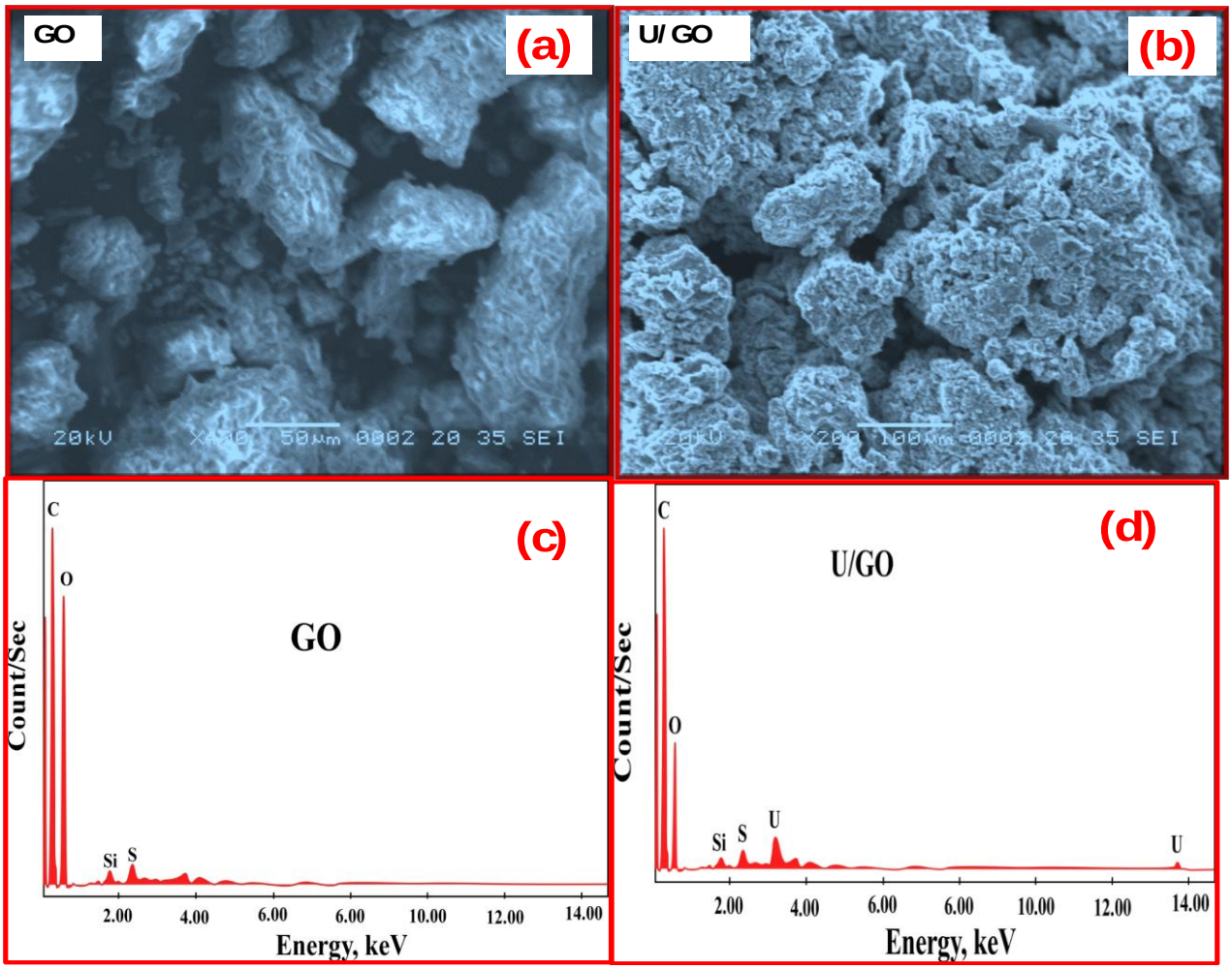

Figure -2: (a) SEM of GO, (b) SEM of UGO/U, (c) EXD of GO, (d) EDX of GO/U.

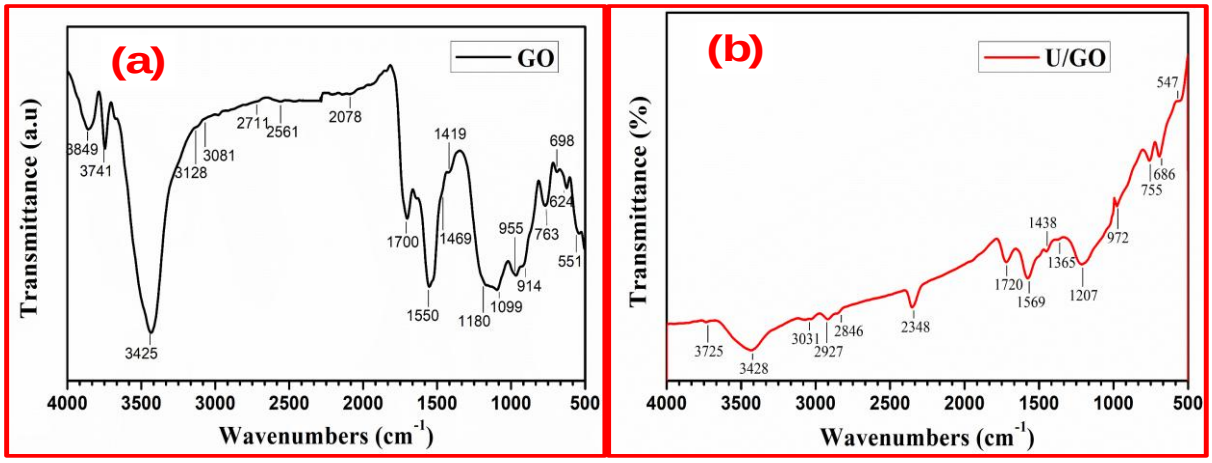

Figure -3: (a) FTIR spectrum of GO, (b) FTIR spectrum of UGO/U.

3.2 U(VI) Adsorption on GO

In the current study, the U(VI) adsorption was fulfilled on graphene oxide (GO), as the adsorbed material from uranyl sulfate ionsin the synthetic solution. Several experiments were conducted on uranium adsorption efficiency to optimize the impact of pH value, contact time, adsorbent dose, initial uranium ions concentration, and temperature.

3.2.1 Effect of pH

The pH of the aqueous solution is the most critical variable affecting metal adsorption on the studied adsorbent. The outcome of pH on the adsorption of uranium onto GO, was studied in various pH values range from 1 to 6 at fixed settings of 50 mg of adsorbent dose and 50 mL of synthetic solution assaying 150 mg/L of uranium ions for 30 min contact time at room temperature. The adsorption uptake of U(VI) as a pH function was offered in Figure 4. The uranium adsorption uptake was increased from 11to 60 mg/g with increasing the solution pH from 1 to 4. Subsequently, the pH increase until 6 led to decreased uranium adsorption uptake to 12mg/g for GO. Thus, the maximum adsorption efficiency of uranium was attained at pH 4.

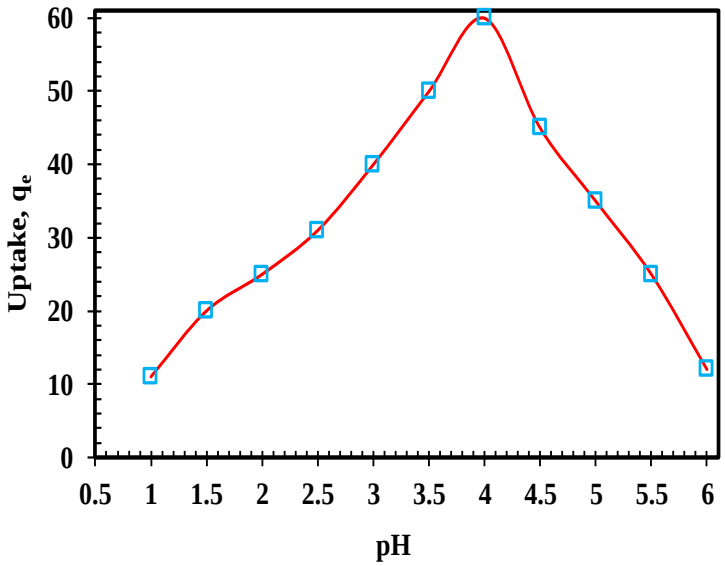

Figure -4:Effect of pH on the uptake capacity of U(VI) by GO (50 mL of 150 mg/L U(VI), 50mg adsorbent dose, 30 min contact time, room temperature).

3.2.2 Effect of Contact Time

The influence of contact time on the adsorption uptake of uranium ions was recognized on GO adsorbent at different contact time varying from 5 to 120 min; however, the other experimental settings were pH4, 50 mL of 150 mg/L U(VI) aqueous solution, 50mg adsorbent dose at room temperature (Figure 5). From the given data, the uranium ions' adsorption uptake was increased from 20 to 68mg/g with increasing the contact time from 5 min to reach the equilibrium of about 50 min. Simultaneously, changing the contact time up to 120 min has no perceptible effect on uranium ions' adsorption uptake. Hence, the contact time of 50 min was suitable for additional adjusting conditions for uranium ions adsorption.

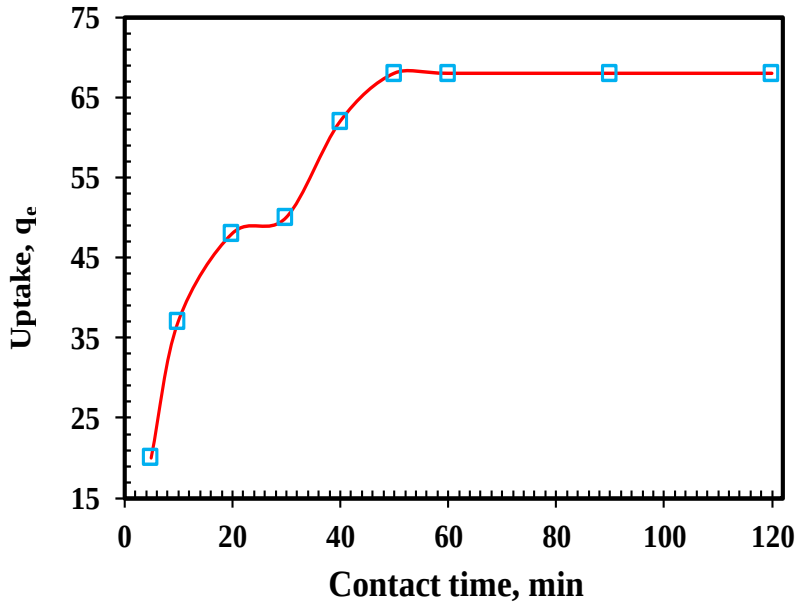

Figure -5:Effect of contact time on the uptake capacity of U(VI) by GO (50 mL of 150 mg/L U(VI), pH4, 50mg adsorbent dose, room temperature).

3.2.3 Effect of Initial Uranium ions Concentration

Initial metalions concentration is the utmost significant parameter on the adsorption system. Several experiments were done to study the effect of initial U(VI) concentration on U(VI) adsorption efficiency using GO adsorbent. These experiments were applied by stirring 50 mL of the standard solution of uranium ions in the range of 25 to 600 mg/L at pH4 with 50 mg of GO adsorbent for 50 min contact time at room temperature. The results in Figure 6 revealed that the initial uranium ions concentration increased, the adsorption efficiency increased, and it reached a maximum loading at 150 mg/L initial uranium concentration. The maximum loading efficiency at 150 mg/L initial uranium concentration for GO adsorbent. Therefore, the uranium maximum loading capacity on GO was 68 mg/g. After that, the uranium ions uptake stayed constant. It expressed that the studied adsorbent reached the maximum loading capacity (saturation capacity)because the mobility of uranyl ions $(UO_2)^{2+}$ in the solutions was the highest, and all active sites of the studied adsorbent filled and blocked with uranyl ions from the solution.

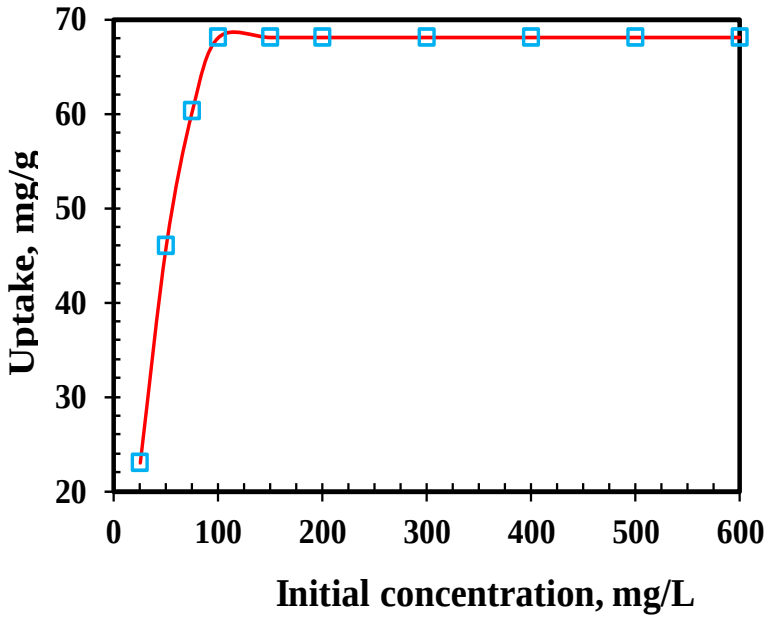

Figure -6:Effect of initial uranium ions concentration on U(VI) adsorption uptake by GO (50 mL volume, pH4,50mg adsorbent dose, 50 min contact time, room temperature).

3.2.4 Effect of Temperature

The effect of temperature on the U(VI) adsorption uptake was fulfilled on GO within range of 25–55 °C, under other experimental aspects were kept constant at solution pH 4, 50mg adsorbent dose, and 50 mL of the aqueous solution containing 150 mg/L of uranium ions for 50 min contact time. The results were exposed in Figure 7, and the uptake capacity decreased from 68mg/g at 25 °C to 64.65 mg/g at 55 °C. It was possibly due to the increase of temperature that might lead to the decomposition of functional groups for GO adsorbent. It might also decrease the active sites of adsorbent; therefore, the adsorption of uranium ions was reduced. The results implied that the adsorption reaction was not associated with energy, and it was an exothermic reaction. Therefore, the room temperature was the optimum temperature for uranium ions' adsorption on GO.

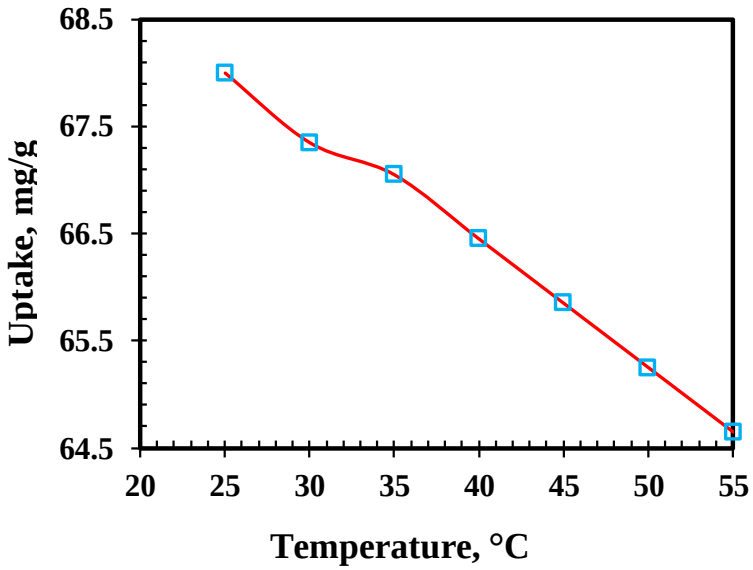

Figure -7: Effect of temperature on U(VI) adsorption uptake by GO (50 mL of 150 mg/L U(VI), pH4,50mg adsorbent dose, 50 min contact time).

3.2.5 Adsorption Kinetics

The adsorption kinetics is one of the most critical data to realize the adsorption mechanism and measure the solid adsorbents' performance. Lagergren's pseudo-first-order and pseudo-second-order models were utilized for the investigational data to calculate the adsorption kinetics of uranium ions on GO adsorbent. The linearized formula of the pseudo-first-order kinetics as the following equation (Su et al., 2021):

$$\log\left(q_e - q_t\right) = \log q_e - \left(\frac{k_1}{2.303}\right)t \qquad (3)$$

Where q_e and q_t(mg/g) are the amounts of uranium ions adsorbed at equilibrium and at time t (min), and k_1 (1/min) is the pseudo-first-order rate constant. A relation of log(q_e–q_t) against t was applied, and the rate constant k_1 and q_e were estimated from the slope and intercept. The data in Figure 8 and Table 1 manifested that the correlation coefficient R^2 and $q_{e(cal)}$ values for the adsorption processes did not match the pseudo-first-order kinetic model. The conclusion is that uranium ions' adsorption onto GO did not fit for the pseudo-first-order reaction. Conversely, the pseudo-second-order kinetic model was applied and presented in the following (Su et al., 2021):

$$\frac{t}{q_t} = \frac{1}{k_2 q_e^{\,2}} + \left(\frac{1}{q_e}\right)t \qquad (4)$$

Where k_2 (g/mg.min) is the rate constant of the pseudo-second-order, q_t (mg/g) is the uranium ions amount adsorbed at time t (min), and q_e is the U(VI) amount at equilibrium (mg/g). This kinetic model was further probable to predict adsorption's kinetic behavior through chemical adsorption that the rate-controlling step. The plot of t/q_t vs. t would provide a straight line. The $q_e$and $k_2$were calculated from the slope and intercept of the plot. From the data in Figure 10, the plot was the straight line of GO with an excellent correlation coefficient close to unity, representing the applicability of the pseudo-second-order model (Table 1). The calculated uptake value obtained from this model (q_{cal}) was relative to the experimental uptake (q_{exp}) at equilibrium time. The data proposed that the uranium ions' adsorption onto GO was followed well the pseudo-second-order kinetic.

Table -1: Kinetic parameters for U(VI) ions adsorption on GO adsorbent.

Kinetic models	Parameters	GO
Pseudo-first-order	**q_e (mg/g)**	**59.67**
	k_1 (1/min)	**0.050**
	R^2	**0.917**
Pseudo-second-order	**q_e (mg/g)**	**76.33**
	k_2 (g/mg min)	**1.17×10^{-3}**
	R^2	**0.992**
Experimental uptake	**q_{exp}**	**68.00**

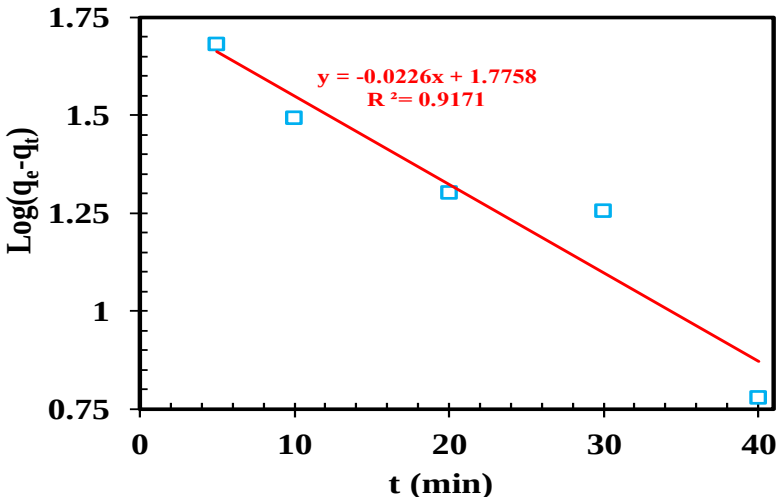

Figure -8: Pseudo-first order kinetic model for U(VI) adsorption on GO adsorbent.

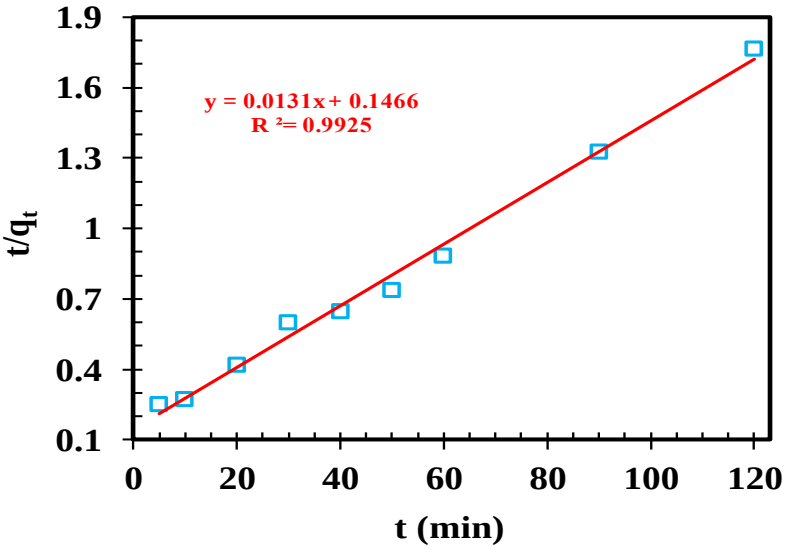

Figure -9: Pseudo-second order kinetic model for U(VI) adsorption on GO adsorbent.

3.2.6 Adsorption Isotherms

Adsorption isotherms are crucial to realize the information around adsorption mechanism, adsorbent surface properties, and other parameters affected in adsorption procedures. The adsorption isotherm is the relation between U(VI) adsorbed on a unit mass of adsorbent from the aqueous phase and its concentration at a fixed temperature. The adsorption isotherm is the elementary condition for designing the adsorption scheme (Cheira et al., 2014b). The adsorption experiments were applied at the optimum settings to scrutinize the good fitting isotherm model. The Langmuir, and Freundlich, models were employed to determine the suitable isotherm and their capability to relate the investigational data.

The Langmuir model assumes that the U(VI) uptake comes to pass on a homogeneous surface through a saturated monolayer adsorbent surface with uranium ions. The adsorption energy is fixed; besides, there is no transmission of the uranium ions on the surface plane (Kadous et al., 2010). The Langmuir isotherm was stated through the following equation:

$$\frac{C_e}{q_e} = \frac{1}{q_{\max} b} + \left(\frac{1}{q_{\max}}\right) C_e \qquad (5)$$

Where C_e (mg/L) is the U(VI) concentration in the aqueous phase at equilibrium, q_e (mg/g) is the amount of U(VI) adsorbed for each unit mass of adsorbent at equilibrium, andq_{max} (mg/g) is the maximum amount of U(VI) adsorbed per unit mass of adsorbent for a whole monolayer, as well as *b*, is a constant correlated to the binding sites' affinity and the adsorption energy (L/mg). Therefore, the linear plot of C_e/q_e vs. C_e was displayed in Figure10. From Table 2, the maximum uptake (68.49mg/g) was closer to experimental uptake (68.00 mg/g). The correlation coefficient (R^2) is near to unity for GO adsorbent. These results designated that the U(VI) adsorption procedure obeyed Langmuir isotherm, and it inferred that the studied adsorbent was homogeneous in aqueous solutions.The attained data displayed that the adsorption system was followed the Langmuir isotherm.

However, the Freundlich isotherm designates the uranium ions' adsorption on the solid surface. It is typically used to explain the surface energies and heterogeneity (Kadous et al., 2010). The Freundlich isotherm was set as the following equation:

$$\log q_e = \log K_f + \frac{1}{n} \log C_e \qquad (6)$$

Where, K_f (mg/g) is the Freundlich constant, correlated to overall U(VI) uptake, *n* is the constant related to surface heterogeneity, q_e (mg/g) is the amount of U(VI) adsorbed at equilibrium, and C_e is the U(VI) concentration in the aqueous solution at equilibrium. The plotting of logq_e vs. logC_e received a regression line that led to calculating *n* and K_f values. The values of the Freundlich constants K_f and *n* calculated from the intercept and the slope, (Figures 11) and the adsorption parameters were displayed in Table 2. K_f(mg/g) value was lower than the experimental uptake for GO adsorbents; besides, the correlation coefficient was 0.635. From the achieved data, it was exposed that the experimental data did not fit the Freundlich isotherm.

Table -2: Isotherm parameters for U(VI) adsorption on GO adsorbent.

Isotherm models	Parameters	GO
Langmuir isotherm	q_{max} (mg/g)	68.49
	b (L/mg)	0.014
	R^2	0.999
Freundlich isotherm	K_f (mg/g)	32.64
	n (mg.min/g)	7.16
	R^2	0.635
Experimental uptake	q_{exp}	68.00

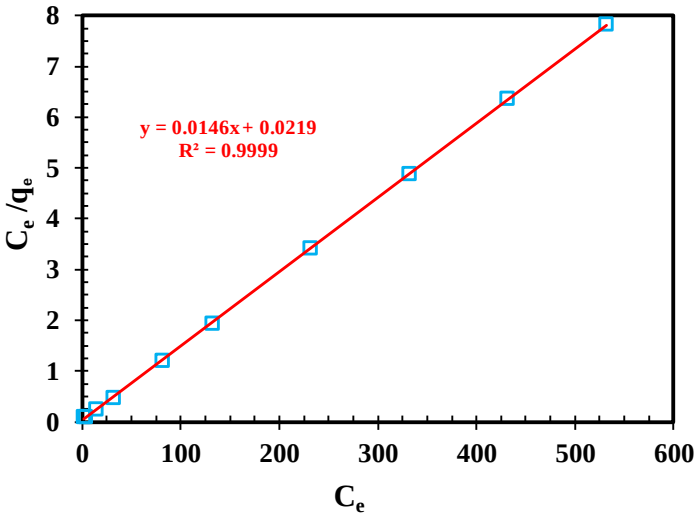

Figure -10: The Langmuir isotherm model of U(VI) adsorption on GO adsorbent.

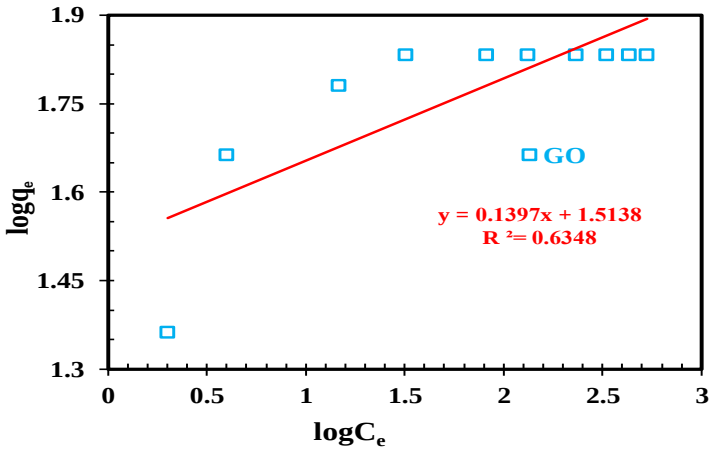

Figure -11: The Freundlich isotherm model of U(VI) adsorption on GO adsorbent.

3.2.7 Thermodynamic Investigations

The mechanism of adsorption is also determined through thermodynamic parameters such as Gibbs free energy change (*ΔG*°), enthalpy change (*ΔH*°), and entropy change (*ΔS*°). The thermodynamic equilibrium constant for the uranium ions adsorption (K_d) was calculated from the investigational data.Thermodynamic parameters for the adsorption behavior of uranium ions by GO were evaluated from the Van't Hoff equations (Cheira, 2020b).

$$\log K_d = \frac{\Delta S^\circ}{2.303R} - \frac{\Delta H^\circ}{2303RT} \quad (7)$$

$$\Delta G^\circ = \Delta H^\circ - T\,\Delta S^\circ \quad (8)$$

Where K_d is the adsorption equilibrium constant (*L*/g), *ΔG*° Gibbs free energy of adsorption (kJ/mol), the *ΔH*° enthalpy change of adsorption (kJ/mol), entropy change of adsorption *ΔS*° (J/mol.K), *R* is the universal gas constant (8.314 J/mol.K), and *T* is the absolute temperature (*K*). The thermodynamic parameters of GO adsorbent were proposed by plotting of logK_d against*1/T* (Figure12) that offered a straight line, the values of *ΔH*° and *ΔS*° were estimated from the slope and intercept. The values of *ΔH*°, *ΔS*°, and *ΔG*° for the studied adsorbent were specified in Table 3. The positive *ΔG*° value of GO adsorbent designated that the adsorption process is

non–spontaneous from the achieved results. The progression in $\Delta G°$ value by increasing the temperature inferred that the adsorption technique was unfavorable at the highest temperature. The negative $\Delta H°$ value proposed exothermic of the adsorption process. Similarly, the negative $\Delta S°$ value displayed the feasibility of adsorption and randomness at the adsorbent/solution interface during the adsorption process of U(VI) ions on the GO adsorbent.

Table -3: Thermodynamic parameters of U(VI) adsorption on GO, adsorbent.

Parameters	T, K	GO
ΔG°, kJ/mol	298 K	0.459
	303 K	0.507
	308 K	0.555
	313 K	0.604
	318 K	0.652
	323 K	0.700
	328 K	0.749
ΔH° , kJ/mol		-2.42
ΔS°, kJ/(mol.K)		-0.96 x 10^{-2}

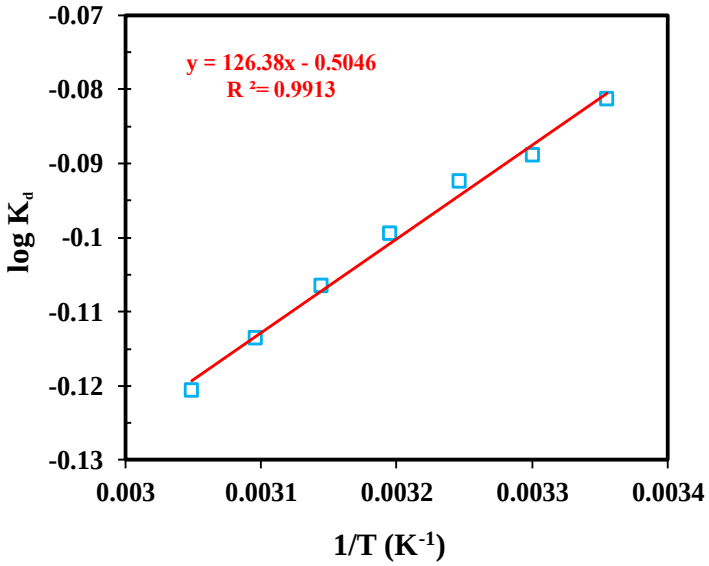

Figure -12: A plot of log K_d against 1/T for U(VI) adsorption on the GO adsorbent.

3.3 Regeneration and Reusability of GO

Regeneration is one of the fundamental characters in the re-reusability of the adsorbents. The uranium-loaded GO (U/GO)was refreshed utilizing 0.8M sulfuric acid solution and 1/50 S/L phase ratio for 60 min contact time at room temperature to reuse the studied GO adsorbent. The adsorption-desorption processes were repeated numerous times till desorption efficiency was diminished to 78% for the GO adsorbent; after seven cycles, it was designated that the choice adsorption establishment of GO adsorbent for uranium recovery.

4. CONCLUSION

The prepared graphene oxide was employed to U(VI) adsorption from sulfate solution. The optimized adsorption conditions were achieved by pH 4, 50 mL of 150 mg/L U(VI), and 50 mg dose for 50 min contact time at room temperature. The recognized maximum uptake of graphene oxide achieved 68.0 mg/g. Additionally, thermodynamic studies were investigated the negative values of $\Delta S°$ and $\Delta H°$ that established a randomness and exothermic performance for U(VI) adsorption, but positive $\Delta G°$ values indicated non-spontaneous adsorption. Moreover, the kinetic suggestions were stated to fit well within the pseudo-second-order kinetic model. The data confirmed that the Langmuir model was suited well for describing adsorption processes. Likewise, the GO adsorbent was indeed regenerated by 0.8M H_2SO_4 and 1/50 S/L ratio for 60 min contact time. The adsorption-desorption processes were repeated numerous times until desorption efficiency was reduced for the GO adsorbent at seven repeated times. It was designated good adsorption of U(VI) on the GO adsorbent.

REFERENCES

Abdien, H.G., Cheira, M.F., Abd-Elraheem, M.A., El-Naser, T.S., Zidan, I.H., 2016a. Extraction and pre-concentration of uranium using activated carbon impregnated trioctyl phosphine oxide. Elixir Appl. Chem. 100, 3462-43469. https://www.elixirpublishers.com/articles/1480509836_ELIXIR2016095352.pdf.

Abdien, H.G., Cheira, M.F., Abd-Elraheem, M.A., Saef El-Naser, T.A., Zidan, I.H., 2016b. Removal of uranium from acidic solution using activated carbon impregnated with tributyl phosphate. Biol. Chem. Res. S.S. Pub. 2016, 313-340. http://www.ss-pub.org/wp-content/uploads/2016/11/BCR2016081701.pdf.

Atia, B., Gado, M., Cheira, M., 2018. Kinetics of uranium and iron dissolution by sulfuric acid from Abu Zeneima ferruginous siltstone, southwestern Sinai, Egypt. Euro-Mediterr. J. Environ. Integr. 3, 39. https://doi.org/10.1007/s41207-018-0080-y.

Atia, B.M., Gado, M.A., Cheira, M.F., El-Gendy, H.S., Yousef, M.A., Hashem, M.D., 2021. Direct synthesis of a chelating carboxamide derivative and its application for thorium extraction from Abu Rusheid ore sample, South Eastern Desert, Egypt. Intern. J. Environ. Anal. Chem. 1-24. https://doi.org/10.1080/03067319.2021.1924161.

Atia, B.M., Khawassek, Y.M., Hussein, G.M., Gado, M.A., El-Sheify, M.A., Cheira, M.F., 2021. One-pot synthesis of pyridine dicarboxamide derivative and its application for uranium separation from acidic medium. J. Environ. Chem. Eng. 9, 105726. https://doi.org/10.1016/j.jece.2021.105726.

Cheira, M.F., El-Didamony, A.M., Mahmoud, K.F., Atia, B.M., 2014a. Equilibrium and kinetic characteristics of uranium recovery by the strong base Ambersep 920U Cl resin. IOSR-Appl. Chem., 7, 32-40. doi:10.9790/5736-07533240.

Cheira, M.F., 2015a. Characteristics of uranium recovery from phosphoric acid by an aminophosphonic resin and application to wet process phosphoric acid. European J. Chem. 6, 48- 56. doi:10.5155/eurjchem.6.1.48-56.1143.

Cheira, M.F.,2015b. Synthesis of pyridylazo resorcinol-functionalized Amberlite XAD-16 and its characteristics for uranium recovery. J. Environ. Chem. Eng. 3, 642-652. https://doi.org/10.1016/j.jece.2015.02.003.

Cheira, M.F., 2019. Synthesis of aminophosphonate-functionalisedZnO/polystyrene-butadiene nanocomposite and its characteristics for uranium adsorption from phosphoric acid. Intern. J. Environ. Anal. Chem. 1-25.https://doi.org/10.1080/03067319.2019.1686493.

Cheira, M.F., 2020a. Solvent extraction of uranium and vanadium from carbonate leach solutions of ferruginous siltstone using cetylpyridinium carbonate in kerosene.Chem. Papers 74, 2247–2266. https://doi.org/10.1007/s11696-020-01073-w.

Cheira, M.F., 2020b. Performance of poly sulfonamide/nano-silica composite for adsorption of thorium ions from sulfate solution. SN Appl. Sci. 2, 398. https://doi.org/10.1007/s42452-020-2221-6.

Cheira, M.F., Atia, B.M., Kouraim M.N., 2017. Uranium (VI) recovery from acidic leach liquor by Ambersep 920U SO_4 resin: Kinetic, equilibrium and thermodynamic studies. J. Rad. Res. Applied Sci. 10, 307-319. https://doi.org/10.1016/j.jrras.2017.07.005.

Cheira, M.F., Kouraim, M.N., Zidan, I.H., Mohamed, W.S., Hassanein, T.F., 2020a. Adsorption of U(VI) from sulfate solution using montmorillonite/polyamide and nano-titanium oxide/polyamide nanocomposites. J. Environ. Chem. Eng. 8, 104427. https://doi.org/10.1016/j.jece.2020.104427.

Cheira, M.F., Mira, H.I., Sakr, A.K., Mohamed, S.A., 2019b. Adsorption of U(VI) from acid solution on a low-cost sorbent: equilibrium, kinetic, and thermodynamic assessments. Nucl. Sci. Tech. 30, 156. https://doi.org/10.1007/s41365-019-0674-3.

Cheira, M.F., Rashed, M.N., Mohamed, A.E., Hussein, G.M., Awadallah, M.A., 2019a.Removal of some harmful metal ions from wet-process phosphoric acid using murexide-reinforced activated bentonite. Mat. Today Chem. 14, 100176.https://doi.org/10.1016/j.mtchem.2019.06.002.

Cheira, M.F., Rashed, M.N., Mohamed, A.E., Zidan, I.H., Awadallah, M.A. 2020b. The performance of Alizarin impregnated bentonite for the displacement of some heavy metals ions from the wet phosphoric acid. Sep. Sci. Tech. 55, 3072-3088. https://doi.org/10.1080/01496395.2019.1675701.

Cheira, M.F., Zidan, I.H., Manaa, E.A., 2014b. Potentiality of white sand for the purification of wet process phosphoric acid from some metallic elements (U, Zn, Cd). Chem. Technol. Indian J. 9(6), 224-233.

Chen, C., Wang, J.L., 2016. Uranium removal by novel grapheneoxide-immobilized Saccharomyces cerevisiae gel beads. J.Environ. Radioact. 162, 134-145. https://doi.org/10.1016/j.jenvrad.2016.05.012.

Cheng, H., Zeng, K., Yu, J., 2013. Adsorption of uranium from aqueous solution by graphene oxide nanosheets supported on sepiolite. J. Radioanal. Nucl. Chem. 298, 599-603. https://doi.org/10.1007/s10967-012-2406-6.

Cheng, J.S., Du, J., Zhu, W.J., 2012. Facile synthesis of three-dimensional chitosan-graphene mesostructures for reactive black 5 removal. Carbohydrate Polymers 88(1), 61-67.https://doi.org/10.1016/j.carbpol.2011.11.065.

Chowdhury, S., Balasubramanian, R., 2014. Recent advances in the use of graphene-family nanoadsorbents for removal of toxic pollutants from wastewater. Adv. Colloid Interf. Sc. 204, 35-56.https://doi.org/10.1016/j.cis.2013.12.005.

Dong, S.N., Sun, Y.Y., Wu, J.C., Wu, B.J., Creamer, A.E., Gao, B., 2016. Graphene oxide asfilter media to remove levofloxacin and lead from aqueous solution. Chemosphere 150, 759-764.https://doi.org/10.1016/j.chemosphere.2015.11.075.

Duff, M.C., Coughlin, J.U., Hunter, D.B., 2002. Uranium co-precipitation with iron oxideminerals. Geochim. Cosmochim. Acta 66, 3533–3547. https://doi.org/10.1016/S0016-7037(02)00953-5.

Gado. M.A., Atia, B.M., Cheira, M.F., Abdou, A.A., 2019. Thorium ions adsorption from aqueous solution by amino naphtholsulphonate coupled chitosan.Intern. J. Environ. Anal. Chem. 1-18. https://doi.org/10.1080/03067319.2019.1683552.

Hassanin, M.A., El-Gendy, H.S., Cheira, M.F., Atia, B.M., 2019. Uranium ions extraction from the waste solution by thiosemicarbazide anchored cellulose acetate. Intern. J. Environ. Anal. Chem. 1-25.https://doi.org/10.1080/03067319.2019.1667984.

Hu, B.W., Hu, Q.Y., Li, X., Pan, H., Tang, X.P., Chen, C.G., Huang, C.C., 2017. Rapid and highly efficient removal of Eu(III) from aqueous solutions using graphene oxide. J. Mol. Liq. 229, 6-14. https://doi.org/10.1016/j.molliq.2016.12.030.

Jiao, X., Zhang, L.Y., Qiu, Y.S., Guan, J.F., 2017. Comparison of the adsorption of cationic blue onto graphene oxides prepared from natural graphites with different graphitization degrees. Colloid Surface A 529, 292-301.https://doi.org/10.1016/j.colsurfa.2017.05.094.

Kadous, A., Didi, M.A., Villemin, D., 2010. A new sorbent for uranium extraction: ethylenediaminotris-methylene phosphonic acid grafted on poly styrene resin. J. Radioanal. Nucl. Chem. 284, 431-438. https://doi.org/10.1007/s10967-010-0495-7.

Kim, J., Cote, L.J., Kim, F., Yuan, W., Shull, K.R., Huang, J.X., 2010. Graphene oxide sheets at interfaces. J. Am. Chem. Soc. 132(23), 8180-8186.https://doi.org/10.1021/ja102777p.

Kim, S., Park, C.M., Jang, M., Son, A., Her, N., Yu,M., Snyder, S., Kim, D., Yoon, Y., 2018. Aqueous removal of inorganic and organic contaminants by graphene-based nanoadsorbents: A review. Chemosphere 212, 1104-1124. https://doi.org/10.1016/j.chemosphere.2018.09.033.

Li, J., Zhang, S.W., Chen, C.L., Zhao, G.X., Yang, X., Li, J.X., Wang, X.K., 2012. Removal of Cu(II) and fulvic acid by graphene oxide nanosheets decorated with Fe_3O_4 nanoparticles. ACS Appl. Mater. Interfaces 4(9), 4991-5000.https://doi.org/10.1021/am301358b.

Li, Z.J., Wang, L., Yuan, L.Y., Xiao, C.L., Mei, L., 2015. Efficient removal of uraniumfrom aqueous solution by zero-valent iron nanoparticle and its graphenecomposite. J. Hazard Mater. 290, 26-33. https://doi.org/10.1016/j.jhazmat.2015.02.028.

Liao, Y., Wang, M., Chen, D., 2019. Electrosorption of uranium(VI) by highly porous phosphate-functionalized graphene hydrogel, Applied Surf. Sci. 484, 83–96. https://doi.org/10.1016/j.apsusc.2019.04.103.

Liu, X., Xu, X.T., Sun, J., Alsaedi, A., Hayat, T., Li, J.X., Wang, X.K., 2018. Insight into theimpact of interaction between attapulgite and graphene oxide on the adsorption ofU(VI). Chem. Eng. J. 343, 217–224.https://doi.org/10.1016/j.cej.2018.02.113.

Marczenko, Z., Balcerzak, M., 2000. Separation, Preconcentration and Spectrophotometry in Inorganic Analysis. Elsevier Science B.V., Amesterdam, Netherland. 446-455.

Sakr, A.K., Mohamed, S.A., Mira, H.I., Cheira, M.F., 2018. Successive leaching of uraniumand rare earth elements from el Sela mineralization. J. Sci. Eng. Res. 5, 95–111. https://jsaer.com/archive/volume-5-issue-9-2018/.

Sanchez, V.C., Jachak, A., Hurt, R.H., Kane, A.B., 2012. Biological interactions of graphene-family nanomaterials: An interdisciplinary review. Chem. Res. Toxicol. 25(1), 15-34. https://doi.org/10.1021/tx200339h.

Sayed, A.S., Abdelmottaleb, M., Cheira, M.F., Abdel-Aziz, G., Gomaa, H., Hassanein, T.F., 2020. Date seed as an efficient, eco-friendly, and cost-effective bio-adsorbent for removal of thorium ions from acidic solutions. Aswan Uni. J. Environ. Studies 1, 106-124. doi: 10.21608/aujes.2020.124579.

Su, M., Liu, Z., Wu, Y., Peng, H., Ou, T., Huang, S., Song, G., Kong, L., Chen, N., Chen, D., 2021. Graphene oxide functionalized with nano hydroxyapatite for the efficient removal of U(VI) from aqueous solution. Environ. Pollution 268, 115786. https://doi.org/10.1016/j.envpol.2020.115786.

Wang, C., Li, H., Liao, S.H., Zheng, H., Wang, Z.Y., Pan, B., Xing, B.S., 2013. Coadsorption, desorption hysteresis and sorption thermodynamics of sulfamethoxazole and carbamazepine

on graphene oxide and graphite. Carbon 65, 243-251.https://doi.org/10.1016/j.carbon.2013.08.020.

Wang, J., Chen, B.L., 2015. Adsorption and coadsorption of organic pollutants and a heavy metal by graphene oxide and reduced graphene materials. Chem. Eng. J. 281, 379-388.https://doi.org/10.1016/j.cej.2015.06.102.

Yao, W., Wang, X.X., Liang, Y., Yu, S.J., Gu, P.C., Sun, Y.B., Xu, C., Chen, J., Hayat,T., Alsaedi, A., Wang, X.K., 2018. Synthesis of novel flower-like layered double oxides/carbondots nanocomposites for U(VI) and 241 Am(III) efficient removal: batch and EXAFSstudies. Chem. Eng. J. 332, 775–786.https://doi.org/10.1016/j.cej.2017.09.011.

Zaaba, N.I., Foo, K.L., Hashim, U., Tan, S.J., Liu, W., Voon, C.H., 2017. Synthesis of graphene oxide using modified Hummers method: solvent influence. Procedia Eng. 184, 469 – 477. https://doi.org/10.1016/j.proeng.2017.04.118.

Zhou, C., Ontiveros-Valencia, A., Cornette de Saint Cyr, L., Zevin, A.S., Carey, S.E., Krajmalnik-Brown, R., Rittmann, B.E., 2014. Uranium removal and microbial communityin a H_2-based membrane biofilm reactor. Water Res. 64, 255–264.https://doi.org/10.1016/j.watres.2014.07.013.

Zidan, I.H., Cheira, M.F., Bakry, A.R., Atia, B.M., 2020. Potentiality of uranium recovery from G. Gattar leach liquor using Duolite ES-467 chelating resin: Kinetic, thermodynamic and isotherm features. Intern. J. Environ. Anal. Chem. 1-23. https://doi.org/10.1080/03067319.2020.1748613.

Zong, P.F., Wang, S.F., Zhao, Y.L., Wang, H., Pan, H., He, C.H., 2013. Synthesis andapplication of magnetic graphene/iron oxides composite for the removal ofU(VI) from aqueous solutions. Chem. Eng. J. 220, 45-52.https://doi.org/10.1016/j.cej.2013.01.038.